Ex vivo Confocal Microscopy of Human Corneal Nerves

Mouhamed Al-Aqaba, Thaer S Alomar, Ammar Miri, Usama Fares, Ahmad Muneer Otri, Harminder Singh Dua

Title: Ex vivo Confocal Microscopy of Human Corneal Nerves

Authors: [1]Mouhamed A. Al-Aqaba, MB ChB, FICO; [1]Thaer Alomar, FRCS;[1]Ammar Miri, MD; [1]Usama Fares, MD; [1]Ahmad Muneer Otri, MD;[1]Harmnider S. Dua, MD, PhD.

Affiliations:

[1]Division of Ophthalmology and Visual Sciences, Queen's Medical Centre, the University of Nottingham, U.K.

Key words: Ex-vivo Confocal Microscopy, corneal nerves, Limbal nerves

No of Words: 2680

Abstract Word count: 249

Corresponding author: Prof. Harminder S Dua

Division of Ophthalmology and Visual Sciences

B Floor, Eye and ENT Centre

Queen's Medical Centre

University Hospital, Derby Road

Nottingham NG7 2UH, UK.

Harminder.dua@nottingham.ac.uk

Competing Interest: None declared.

ABSTRACT

Aims: To evaluate the distribution, morphometry and the post-mortem changes of the central and peripheral human corneal nerves by ex-vivo laser-scanning confocal microscopy (EVCM).

Methods: 24 eyes from 14 cadavers were retrieved at different time intervals after death and examined by EVCM. Five regions were examined in each eye namely central, superior, inferior, temporal and nasal. In each region, corneal nerve images were categorized according to their anatomical location in the cornea into sub-basal, stromal and limbal nerves. Five nerve parameters were measured; density, orientation, diameter, numbers and branching pattern.

Results: Ex-vivo confocal scanning of a motionless eye allows high quality imaging and tracking of corneal and limbal nerves. Stromal nerves from the sub-Bowman's plexus perforate the Bowman's zone and terminate in blub like structures, from each of which a leash of sub-basal nerves arise. Following death, sub-basal nerve parameters showed significant changes. The density decreased from 9.23±4.48 to 0.45±0.07 mm/mm^2; the diameter from 4.01±0.81 to 2.08±0.20 μm; the numbers from 8.3 to 1.0 and branching pattern from 39.38% to 0% ($p<0.05$) from day one to day five post-mortem. Stromal and limbal nerves showed no significant changes in their density and diameter.

Conclusions: This study establishes a direct link between sub-basal nerves and the sub-Bowmans nerves via distinct terminal bulbs. Limbal nerves are the thickest, are seen in all quadrants and can be traced to the corneal centre. The sub-basal nerve plexus rapidly degenerates after death but stromal and limbal nerves survive during the first five days after death.

INTRODUCTION

The human cornea is one of the most richly innervated structures in the body and is richly supplied by sensory and autonomic nerves deriving primarily from the ophthalmic division of trigeminal nerve.[1-11] Radially oriented nerve fibre bundles enter the mid stroma at the limbus and give rise to branches that innervate the anterior and mid-stroma. Under Bowman's layer, they form a loose plexus wherefrom branches perforate Bowman's zone and form the sub-basal nerve plexus, fibres from which terminate within the superficial epithelial cells.

Corneal nerves have been studied extensively by light and electron microscopy utilizing different histochemical [12-14] and immunohistochemical [15-19] methods. However, these techniques require the tissue samples to sectioned so considerable information about their spatial arrangement is often lost. [20] Confocal microscopy has offered an unparalleled opportunity to study corneal nerves in vivo[21-24] but is limited by the small field of view and normal microscaddic eye movements affect the image quality. Most in-vivo studies have reported descriptions of nerves in the central cornea. To study corneal nerves in more detail and over a larger area, we considered the possibility of ex vivo confocal examination of freshly obtained cadaver eyes. This eliminated artifacts due to involuntary eye movements and also allowed provided information on the degeneration pattern of human corneal nerves over time.

MATERIALS AND METHODS

The research was approved by the local Research Ethics Committee. 24 post-mortem eyes from 14 patients (7 Women, 7 men), mean age of 76.5 years (range 60-92 years) were

obtained by enucleation at different time intervals after death. The specimens were collected in the period between April 2008 and August 2009. All eyes were considered unsuitable for transplantation due to lack of consent, delayed time to enucleation, cancer related deaths or patients with cognitive disorders. The orientation of the eyes was marked prior to enucleation. The research followed the tenets of the Declaration of Helsinki.

For the purpose of evaluation of post-mortem corneal nerve changes, the eyes were classified into five groups based on the time of enucleation and examination after death; 4 eyes were examined within 24 hours after death (group one), 7 eyes between 24-48 hours (group two), 7 eyes between 2-3 days (group three), 4 eyes between 3-4 days (group four) and 2 eyes between 4-5 days (group five).

Confocal microscopy examination

Immediately after enucleation, the eyes were transferred in sterile Dulbecco's phosphate buffered saline solution (Sigma-Aldrich, UK) to the examination room. The eyes were examined by laser scanning confocal microscope (Heidelberg Retina Tomograph II Rostock Corneal Module [RCM]; Heidelberg Engineering GmbH, Heidelberg, Germany).

To facilitate the examination, the whole globe was held in front of the microscope by a clamp holder specifically designed for such purpose. This had 3 joints (including one ball-and-socket joint) which allowed accurate positioning and orientation of the eye for examination (figure included for Reviewers only). Pressure free contact with the cornea was monitored during the examination using a colored digital camera system that gives a side view of the microscope objective and eye. The average time for examining each eye was about 30 minutes.

Image Analysis

To study both the central and peripheral corneal nerves, five regions were examined sequentially in each eye. These were central, superior, inferior, temporal and nasal. The central area of 5 x 5 square millimeters (sq. mm) was considered as the central region. The side camera of the confocal microscope was used to ensure exact positioning. As the cadaver eyes lacked any natural micro-saccadic movements it was possible to precisely locate the confocal microscope probe. Moreover, identification of the palisade structures provided morphological localization of the limbus. Any nerves located in the palisade region were classed as limbal nerves. Nerves located central to the limbus but outside the 5 x 5 sq. mm central zone of the cornea were classed as peripheral nerves. It was also possible to track the peripheral mid-stromal nerves towards the limbus. These were characterized by thicker hyper-reflective nerve bundles situated within a homogenous hypo-reflective stroma, occasional hyper-reflective clump like structures, dark striae and absence of normal stromal and keratocyte architecture. Some of these limbal stromal IVCM features have been reported previously.[25]

In each region, corneal nerve images were categorized according to their anatomical location within the cornea, into sub-basal, stromal and limbal. Each image was then analysed using image processing and analysis software programs (GNU Image Manipulation Program (GIMP) version 2.6.2; Free Software Foundation, Inc., Boston, MA) and (Image J V.1.31, Wayne Rasband, Research Services Branch, National Institute of Mental Health, Bethesda, Maryland, USA). The software applications were used to measure corneal nerve length and diameter (in pixels) and orientation (in degrees). A plugin software called NeuronJ was used with ImageJ to facilitate the tracing and quantification of corneal nerves semi-manually (figure 1)[26]. Different parameters, adopted from previous studies,[21, 27] were used to analyze corneal nerves:

1. Nerve fibre density (NFD): total length of all nerve fibres and branches within a frame in mm per mm^2.

2. Thickness: the frame was zoomed in on the monitor to 200% and five measurements of the width for sub-basal nerve fibres and three measurements for stromal and limbal nerves were taken.

3. Orientation: the mean value of the angle formed by the nerves with respect to the horizontal plane. Orientation of a nerve was horizontal (if the angle measured between 0^o and 30^o), oblique (between 31^o and 60^o) or vertical (between 61^o and 90^o) (figure 2). For the sub-basal plexus, the main nerve fibres rather than their interconnecting twigs were considered for orientation.

4. Number of nerves: defined as the sum of the nerve branches observed within a frame.

5. Branching patterns within the frame: expressed as the percentage of branches per total number of nerve fibres within a single frame.

Statistical Analysis

Data were analyzed using an analysis tool pack for Microsoft Excel 2007 (Microsoft Corp.), SPSS 16.0 (SPSS, Chicago, IL). A p value of < 0.05 was taken as the threshold of statistical significance. One way repeated measures analysis of variance (ANOVA) was performed to investigate the differences in the corneal nerve parameters among the five groups. The Student's t-test for independent samples was used to establish whether any differences between stromal and limbal nerve diameter were significant.

RESULTS

A total of 366 images were selected. The average number of frames per eye was 15. The distribution of images according to their location within the corneal layers and topography was as follows: 94 images (25%) were of sub-basal nerves, 218 images (60%) were of stromal nerves and 54 images (15%) were of limbal nerves. As far as topographical distribution of images was concerned, 71 images (19%) were from the central cornea, 61 images (17%) were from the superior cornea, 78 images (21%) were from the inferior cornea, 83 images (23%) were from the nasal cornea and 73 images (20%) were from the temporal cornea.

Post-mortem changes (table 2.1)

1. Sub-basal nerves

Density. The density of sub-basal nerves in group one was measured at 9.23±4.48 mm/mm^2. Thereafter it showed a significant decline in group two (4.44±3.56 mm/mm^2) ($p<0.05$). However, no significant changes were observed among groups two, three and four. In group five, the sub-basal nerve density was 0.45±0.07 mm/mm^2 ($p<0.05$).

Diameter. The average sub-basal nerve diameter was measured at 4.01±0.81 μm in group one which then significantly decreased to 3.26±0.78 μm in group two. No statistically significant change was observed in the diameter of sub-basal nerves among groups two, three & four respectively. Thereafter, the diameter of sub-basal nerves showed a significant decrease to 2.08±0.20 μm ($p<0.05$).

Number. The mean number of nerves in group one was 8.3 which then significantly declined to 3.83 in group two ($p<0.05$). No statistically significant change was observed in the number of sub-basal nerves among groups two, three & four respectively. The average number of nerves in group five was 1.00 ($p<0.05$).

Branching pattern. In group one, branching pattern was 39.38 ± 25.52% (figure 3 A & B) which then showed a significant decrease to 17.23 ± 22.32% in groups two ($p<0.05$). No statistically significant difference was noted in branching pattern among groups two, three & four respectively. No nerve branches were observed in group five (figure 4 A & B) ($p<0.05$). Advanced degeneration was characterized by loss of continuity and granularity of the sub-basal nerves (figure 5 A & B).

An interesting and novel observation was that sub-basal nerves terminated in bulb-like or rounded bright structures just above the level of Bowman's zone (figure 6 A & B). These were present as clusters of 2 to 6 bulbs. Converging posterior extensions from bulbs of each cluster terminated in a large stromal nerve trunk. Volume scanning of the region related to these clusters revealed that they were in continuation with anterior stromal (sub-Bowman's) nerves (Movie clips 1, 2, 3 and 4). These bulbs survived longer than the nerves that originated from them. At places blubs could be seen with no fibres emanating from them.

2. Stromal and limbal nerves

Stromal and limbal nerves were detected in all regions examined.

Density & diameter. No significant changes were observed in the density and the diameter of stromal and limbal nerves over 5 days post-mortem. Furthermore, both types of nerves showed no obvious signs of degeneration e.g. granularity or loss of continuity. The average stromal nerve density was 1.77 ± 0.79 mm/mm^2 and the average diameter was 8.58 ± 3.1 μm.

Tracing of corneal nerves from the centre of the cornea towards the periphery showed a gradual increase in the diameter of stromal nerves. The average diameter of stromal nerves in the central cornea was 7.75 ± 2.38 μm while their average diameter in the peripheral cornea

was 8.84 ± 3.27 μm. At the extreme periphery, limbal nerves were the largest nerves observed throughout the cornea. They measured up to 60 μm in diameter (average was 27.60 ± 9.7 μm) which were significantly larger than stromal nerves ($p<0.05$). Figure 7 shows the variation in the thickness of corneal nerves in different layers within the cornea.

Table 1 The results of post-mortem quantitative ex vivo confocal microscopy of human corneal nerves.

Group	Sub-basal nerves				Stromal nerves		Limbal nerves	
	Density (mm/mm^2) mean±SD	Diameter (μm) mean±SD	No. of nerves mean±SD	Branching pattern (%) mean±SD	Density (mm/mm^2) mean±SD	Diameter (μm) mean±SD	Density (mm/mm^2) mean±SD	Diameter (μm) mean±SD
Group one	9.23±4.48	4.01±0.81	8.30±4.5	39.38±25.52%	1.98±1.02	9.48±3.91	3.43±0.64	20.82±10.07
Group two	4.44±3.56	3.26± 0.78	3.83±3.54	17.23±22.32%	1.80±0.86	8.23±3.00	2.48±0.77	27.63±10.78
Group three	3.74±3.27	3.03±0.93	3.65±2.69	16.54±21.10%	1.84±0.73	9.00±3.14	2.58±0.78	23.40±7.95
Group four	3.47±3.49	3.30±0.61	2.37±2.22	14.14±20.00%	1.46±0.58	8.08±2.93	2.05±0.50	22.68±9.28
Group five	0.45±0.07	2.08±0.20	1.00±0.00	0%	1.69±0.75	8.29±2.88	2.43±0.85	25.83±6.87

Group one = within 24 hours post-mortem, group two = 24-48 hours post-mortem, group three = 2-3 days post-mortem, group four = 3-4 days post-mortem, group five = 4-5 days post-mortem.

Orientation of corneal nerves

The orientation of sub-basal, stromal and limbal nerves in the five different topographical areas within the human cornea is shown in Table 2. The majority of the sub-basal nerves were oriented obliquely and to a lesser extent vertically, in all corneal regions including nasal and temporal.

Stromal nerves were seen in the central cornea where their orientation was mainly horizontal. Stromal and limbal nerves were arranged predominantly vertically in the superior & inferior corneal regions and predominantly horizontally in the nasal and temporal regions.

Table 2. Orientation of the sub-basal, stromal and limbal nerves in 5 selected topographical areas within the human cornea.

	Sub-basal nerve orientation (%)	Stromal nerve orientation (%)	Limbal nerve orientation (%)
Central cornea	H (10), O (74), V (16)	H (42), O (29), V (29)	Not applicable
Superior cornea	H (29), O (42), V (29)	H (10), O (30), V (60)	H (22), O (56), V (22)
Inferior cornea	H (21), O (46), V (33)	H (15), O (47), V (38)	H (0), O (27), V (73)
Lateral cornea	H (11), O (47), V (42)	H (60), O (35), V (5)	H (68), O (32), V (0)
Medial cornea	H (10), O (45), V (45)	H (61), O (32), V (7)	H (64), O (18), V (18)

H= horizontal, O=oblique, V=vertical.

DISCUSSION

Post-mortem changes of human corneal nerves have been studied elegantly using light microscopy by Muller et al. They reported that thirteen and a half hours after death, the majority of the sub-basal nerve fibres had degenerated or gone.[13] Our study reports the changes in stromal nerves as well and highlights an important structure at the junction of the stromal nerves with the sub-basal plexus. In our study, the sub-basal nerve plexus was the most affected by post-mortem degeneration. The sub-basal nerve branches showed rapid disintegration and the branching pattern significantly declined 24 hours after death. Over the first four days after death, the sub-basal nerves showed a noticeable decrease in the density, diameter and number and they were hardly distinguishable by the fifth day. It is worth noting that degenerated nerves below the resolution of confocal microscope (1 μm) could not be studied. Nevertheless, patchy degeneration was noted from the first day post-mortem. This might explain the results reported by Muller et al who used very small samples of 1-2 mm^2 for en face examination using light microscopy.[13] They could have missed sites where the nerves were present and they completely missed the detection of the bulbs.

The greatest difference in the sub-basal nerve density between group one and two was the rapid degeneration of the nerve branches by the second day post-mortem. This also reflected in the branching pattern. It has been shown that there is a high correlation between the number of nerves and nerve density in all corneal regions.[21] As far as changes in the sub-basal nerves in groups two, three and four are concerned, there was increasing number of areas where total nerve loss was observed with each passing day after death, but in areas where sub-basal nerves were found and measured in these groups, no significant difference

was found in these parameters. It is likely that progressive degeneration continued to occur but was not detectable by confocal microscopy. Nevertheless, the overall structural appearance of the main sub-basal nerves was maintained in parts of the cornea during the first five days post-mortem.

Several confocal studies have shown that the sub-basal nerve density in normal individuals can vary depending on the type of in vivo confocal microscope used. Reported sub-basal nerve densities using laser scanning confocal microscope were as high as 25.9 ± 7.0 mm/mm^2 [28] and 21.6 ± 5.98 mm/mm^2.[29] Nerve diameter in normal individuals ranged from 0.52 ± 0.23 [22] to 4.68 ± 0.68 μm [30]. In our study, the sub-basal nerve density in the first day post-mortem was markedly reduced but the nerve diameter was within the normal range in the nerves that survived. Theoretically, scanning the same corneas over time could possibly give more precise figures but we found that sequential examination of the same specimen resulted in accelerated disintegration and sloughing of the corneal epithelium with injury to the sub-basal plexus. Pathologically, the post-mortem changes can be explained by failure of axon transport resulting in degeneration of vulnerable distal regions of long axons. Degeneration appears to advance proximally toward the nerve cell body (dying-back).[31]

The termination of the sub-basal nerves into characteristic bright bulb-like thickenings and the relation of these structures to underlying stromal nerves in normal corneas is unique to the current study. This strongly correlates with our recent histological demonstration of budding and branching pattern of sub-Bowman's nerves in the anterior stroma.[32] Similar structures were also reported in patients with Fuchs endothelial dystrophy where it was suggested that they related to the disease condition.[20]

We did not notice any obvious signs of structural changes in, or alterations in density and diameter of the stromal and limbal nerves in the first 5 days after death. In one study by Szaflik, corneal nerves including sub-basal nerves were distinguished in 5 days cold preserved corneas from eye bank using white light confocal microscopy.[33]

In our study, the average stromal nerve density was 1.77 ± 0.79 mm/mm^2. This figure was different from the results obtained by other investigators using slit scanning confocal microscope (0.45 ± 0.11 mm/mm^2 [27] and 3.61 ± 1.04 mm/mm^2 [21]). However, our measurement of the average stromal nerve diameter was 8.58 ± 3.1 μm (7.75 ± 2.38 μm centrally, 8.84 ± 3.27 μm peripherally). These (ex vivo post-mortem measurements) are comparable to the results obtained in several in vivo studies using slit scanning confocal microscope (Hosal et al, 9.63 ± 1.88 μm; Benitez del Castillo et al, 7.64 ± 2.54 μm; Oliveira-Soto, 6.3 ± 1.8 μm).[21, 30, 34] Other investigators reported a lower stromal nerve diameter.[27, 35] The variation in the results might be due to different kinds of confocal microscopes used with different light sources and resolution and/or the fact that stromal nerves run obliquely, relative to the en face sections of confocal images. Therefore, obtaining an enface image through the centre of the nerve is not always possible especially when involuntary eye movements are present .[23]

There are no previous estimates of limbal nerve parameters in the literature. It has been reported that scanning corneal limbus for the evaluation of deep structures was not possible due to diffuse light scatter from the sclera particularly if white light confocal microscopy was

used.[25, 36] However, we have managed to scan this region and obtain good quality images of limbal nerves at the extreme periphery of the cornea.

The majority of the main sub-basal nerves were oriented obliquely and to less extent vertically in all corneal regions including nasal and temporal sides, fibres with horizontal orientation being the least. The current study does not support the finding by Muller et al. that the sub-basal nerve bundles in central and mid-peripheral cornea run first in the 9-3 o'clock hour's direction, then after bifurcation in the 12-3 o'clock hours direction and after a second bifurcation again in the 9-3 o'clock hours direction.

In general, the orientation of the stromal and limbal nerves is perpendicular to the corresponding corneo-scleral junction. These nerves enter the cornea from all quadrants and move anteriorly toward the centre of the cornea, giving rise to branches that innervate the anterior and mid-stroma.

In conclusion, this study establishes a direct link between sub-basal nerves and the sub-Bowman's nerves via distinct terminal bulbs. Limbal nerves are the thickest, are seen in all quadrants and can be traced to the corneal centre. The sub-basal nerve plexus rapidly degenerates post-mortem but stromal and limbal nerves survive during the first five days after death.

Licence for Publication

"The Corresponding Author has the right to grant on behalf of all authors and does grant on behalf of all authors, an exclusive licence (or non exclusive for government employees) on a worldwide basis to the BMJ Publishing Group Ltd and its Licensees to permit this article (if accepted) to be published in BJO editions and any other BMJPGL products to exploit all subsidiary rights, as set out in our licence (http://group.bmj.com/products/journals/instructions-for-authors/licence-forms/)."

References

1 Arvidson B. Retrograde axonal transport of horseradish peroxidase from cornea to trigeminal ganglion. *Acta Neuropathol*. 1977;**38**:49-52.

2 Morgan CW, Nadelhaft I, de Groat WC. Anatomical localization of corneal afferent cells in the trigeminal ganglion. *Neurosurgery*. 1978;**2**:252-8.

3 Marfurt CF. The somatotopic organization of the cat trigeminal ganglion as determined by the horseradish peroxidase technique. *Anat Rec*. 1981;**201**:105-18.

4 Marfurt CF, Del Toro DR. Corneal sensory pathway in the rat: a horseradish peroxidase tracing study. *J Comp Neurol*. 1987;**261**:450-9.

5 Morgan C, Jannetta PJ, deGroat WC. Organization of corneal afferent axons in the trigeminal nerve root entry zone in the cat. *Exp Brain Res*. 1987;**68**:411-6.

6 Marfurt CF, Echtenkamp SF. Central projections and trigeminal ganglion location of corneal afferent neurons in the monkey, Macaca fascicularis. *J Comp Neurol*. 1988;**272**:370-82.

7 ten Tusscher MP, Klooster J, Vrensen GF. The innervation of the rabbit's anterior eye segment: a retrograde tracing study. *Exp Eye Res*. 1988;**46**:717-30.

8 Marfurt CF, Kingsley RE, Echtenkamp SE. Sensory and sympathetic innervation of the mammalian cornea. A retrograde tracing study. *Invest Ophthalmol Vis Sci*. 1989;**30**:461-72.

9 Keller JT, Bubel HC, Wander AH, Tierney BE. Somatotopic distribution of corneal afferent neurons in the guinea pig trigeminal ganglion. *Neurosci Lett*. 1991;**121**:247-50.

10 LaVail JH, Johnson WE, Spencer LC. Immunohistochemical identification of trigeminal ganglion neurons that innervate the mouse cornea: relevance to intercellular spread of herpes simplex virus. *J Comp Neurol*. 1993;**327**:133-40.

11 Felipe CD, Gonzalez GG, Gallar J, Belmonte C. Quantification and immunocytochemical characteristics of trigeminal ganglion neurons projecting to the cornea: effect of corneal wounding. *Eur J Pain*. 1999;**3**:31-9.

12 Zander E, Weddell G. Observations on the innervation of the cornea. *J Anat*. 1951;**85**:68-99.

13 Muller LJ, Vrensen GF, Pels L, *et al.* Architecture of human corneal nerves. *Invest Ophthalmol Vis Sci*. 1997;**38**:985-94.

14 Muller LJ, Pels L, Vrensen GF. Ultrastructural organization of human corneal nerves. *Invest Ophthalmol Vis Sci*. 1996;**37**:476-88.

15 Jones MA, Marfurt CF. Calcitonin gene-related peptide and corneal innervation: a developmental study in the rat. *J Comp Neurol*. 1991;**313**:132-50.

16 Toivanen M, Tervo T, Partanen M, *et al.* Histochemical demonstration of adrenergic nerves in the stroma of human cornea. *Invest Ophthalmol Vis Sci*. 1987;**28**:398-400.

17 Tervo K, Tervo T, Eranko L, *et al.* Substance P-immunoreactive nerves in the human cornea and iris. *Invest Ophthalmol Vis Sci*. 1982;**23**:671-4.

18 Tervo T. Consecutive demonstration of nerves containing catecholamine and acetylcholinesterase in the rat cornea. *Histochemistry*. 1977;**50**:291-9.

19 Ueda S, del Cerro M, LoCascio JA, Aquavella JV. Peptidergic and catecholaminergic fibers in the human corneal epithelium. An immunohistochemical and electron microscopic study. *Acta Ophthalmol Suppl*. 1989;**192**:80-90.

20 Guthoff RF, Wienss H, Hahnel C, Wree A. Epithelial innervation of human cornea: a three-dimensional study using confocal laser scanning fluorescence microscopy. *Cornea*. 2005;**24**:608-13.

21 Oliveira-Soto L, Efron N. Morphology of corneal nerves using confocal microscopy. *Cornea*. 2001;**20**:374-84.

22 Grupcheva CN, Wong T, Riley AF, McGhee CN. Assessing the sub-basal nerve plexus of the living healthy human cornea by in vivo confocal microscopy. *Clin Experiment Ophthalmol*. 2002;**30**:187-90.

23 Patel D, McGhee CN. In vivo confocal microscopy of human corneal nerves in health, in ocular and systemic disease, and following corneal surgery: a review. *Br J Ophthalmol*. 2008.

24 Patel DV, McGhee CN. Mapping of the normal human corneal sub-Basal nerve plexus by in vivo laser scanning confocal microscopy. *Invest Ophthalmol Vis Sci*. 2005;**46**:4485-8.

25 Kobayashi A, Sugiyama K. In vivo corneal confocal microscopic findings of palisades of Vogt and its underlying limbal stroma. *Cornea*. 2005;**24**:435-7.

26 Meijering E, Jacob M, Sarria JC, *et al.* Design and validation of a tool for neurite tracing and analysis in fluorescence microscopy images. *Cytometry A*. 2004;**58**:167-76.

27 Simo Mannion L, Tromans C, O'Donnell C. An evaluation of corneal nerve morphology and function in moderate keratoconus. *Cont Lens Anterior Eye*. 2005;**28**:185-92.

28 Patel DV, Ku JY, Johnson R, McGhee CN. Laser scanning in vivo confocal microscopy and quantitative aesthesiometry reveal decreased corneal innervation and sensation in keratoconus. *Eye*. 2008.

29 Niederer RL, Perumal D, Sherwin T, McGhee CN. Corneal innervation and cellular changes after corneal transplantation: an in vivo confocal microscopy study. *Invest Ophthalmol Vis Sci*. 2007;**48**:621-6.

30 Hosal BM, Ornek N, Zilelioglu G, Elhan AH. Morphology of corneal nerves and corneal sensation in dry eye: a preliminary study. *Eye*. 2005;**19**:1276-9.

31 Shin JO. Color Atlas of Nerve Biopsy Pathology. First ed. Florida: CRC Press 2002.

32 Al-Aqaba M, Fares U, Suleman H, *et al*. Architecture and Distribution of Human Corneal Nerves. *Br J Ophthalmol*. 2009;**[Epub ahead of print]**.

33 Szaflik JP. White light confocal microscopy of preserved human corneas from an eye bank. *Cornea*. 2007;**26**:265-9.

34 Benitez del Castillo JM, Wasfy MA, Fernandez C, Garcia-Sanchez J. An in vivo confocal masked study on corneal epithelium and subbasal nerves in patients with dry eye. *Invest Ophthalmol Vis Sci*. 2004;**45**:3030-5.

35 Mocan MC, Durukan I, Irkec M, Orhan M. Morphologic alterations of both the stromal and subbasal nerves in the corneas of patients with diabetes. *Cornea*. 2006;**25**:769-73.

36 Patel DV, Sherwin T, McGhee CN. Laser scanning in vivo confocal microscopy of the normal human corneoscleral limbus. *Invest Ophthalmol Vis Sci*. 2006;**47**:2823-7.

FIGURE LEGENDS

Figure 1. Semi-manual tracing of the sub-basal nerve fibres using a NeuronJ, an imageJ plugin software. (scale bar = 100 μm)

Figure 2. Measurement of the stromal nerve orientation using GNU Image Manipulation Program (GIMP).

Figure 3 (A and B). The appearance of sub-basal nerve plexus in the first day post-mortem. Branching pattern is preserved. (scale bar = 100 μm)

Figure 4 (A and B). Sub-basal nerve plexus shows lack of branches which have largely degenerated by the second day post-mortem. The main sub-basal nerves are also thinner than those observed in figure 3. (scale bar = 100 μm)

Figure 5 (A and B). Advanced degeneration of the sub-basal nerves with loss of continuity (white arrowheads) and granularity (white arrows). (scale bar = 100 μm)

Figure 6 (A and B). Termination of a sub-basal nerves into bright bulb like structures at the level of basal epithelial cells. (scale bar = 100 μm)

Figure 7. Variation in thickness of corneal nerves in different regions within the cornea. (A) sub-basal nerves [4.01 ± 0.81 μm], (B) central stromal nerve [7.75 ± 2.38 μm], (C) peripheral stromal nerve [8.84 ± 3.27 μm] and (D) limbal nerve [27.60 ± 9.7 μm]. (scale bar = 100 μm).

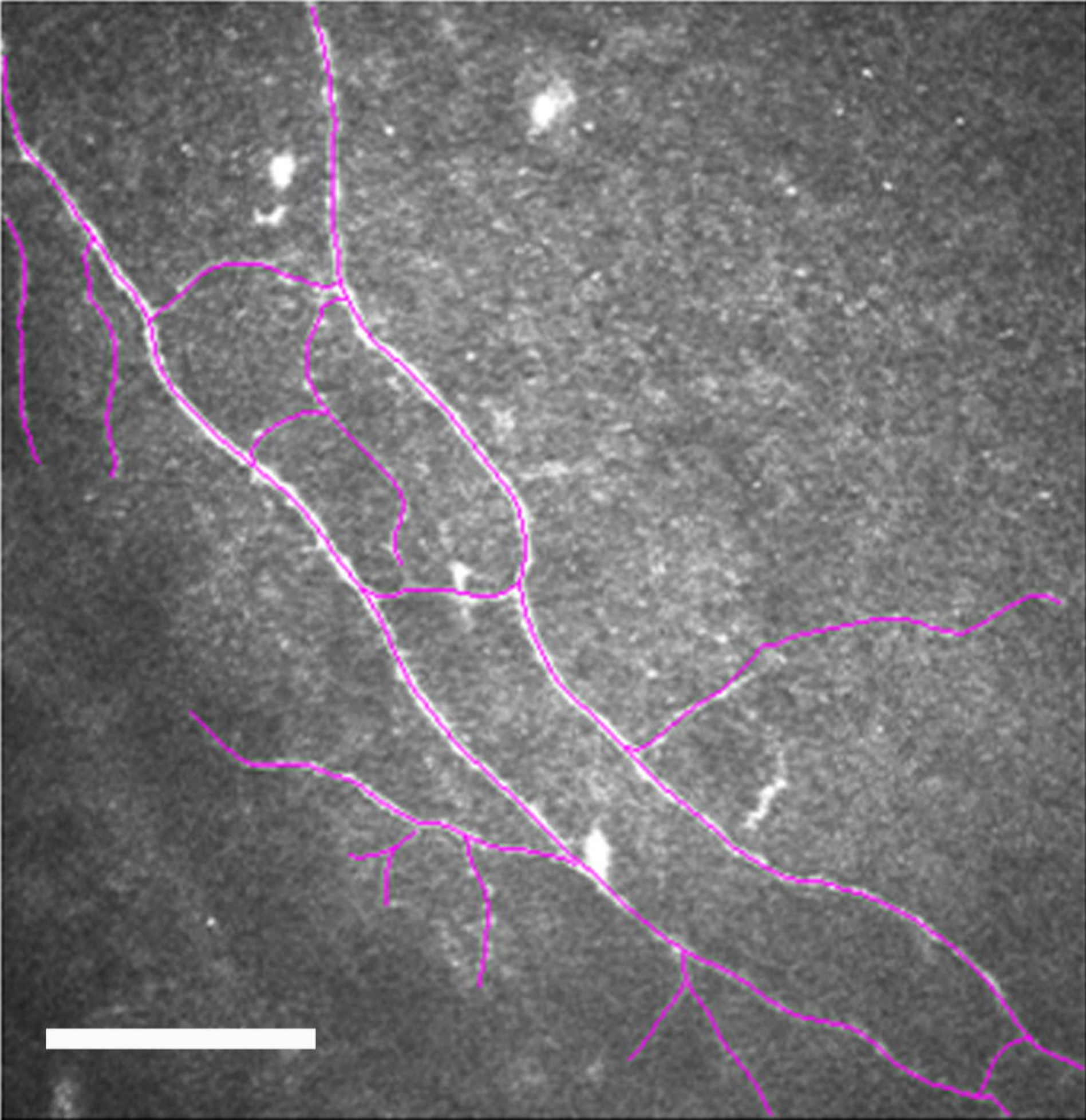

Angle of orientation in degrees

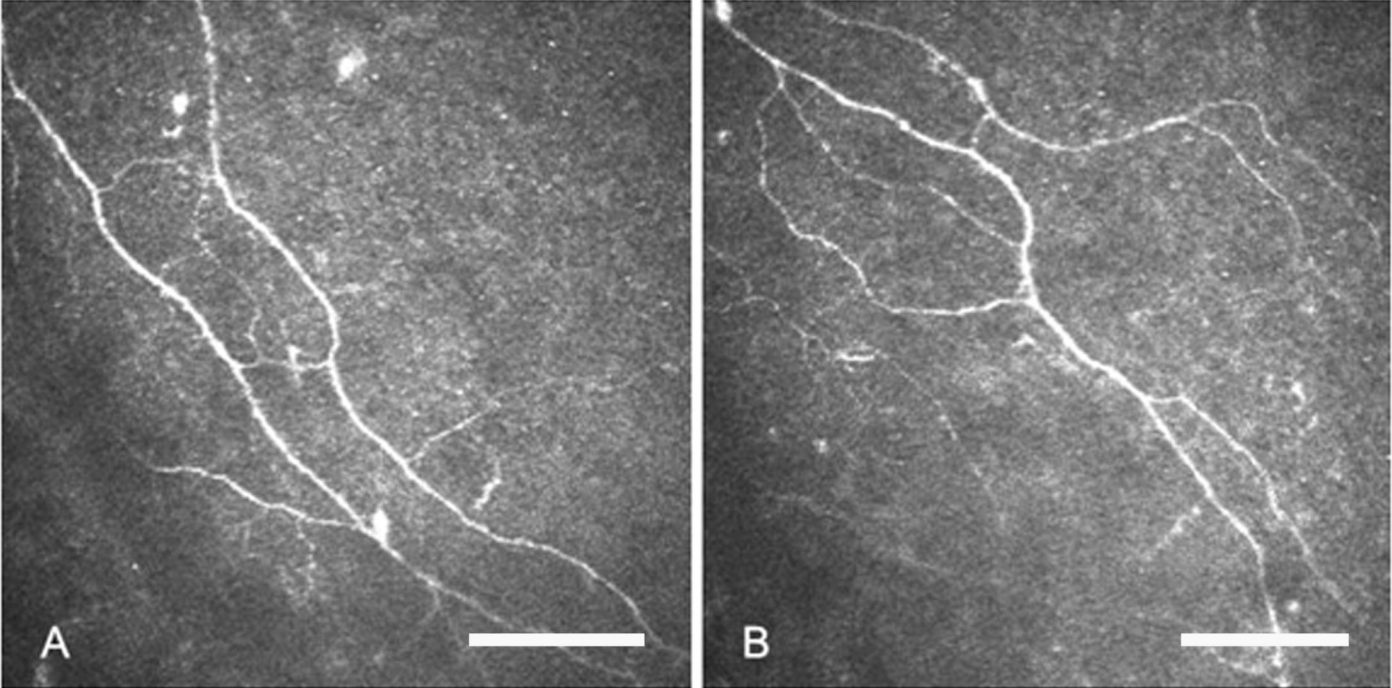
A
B

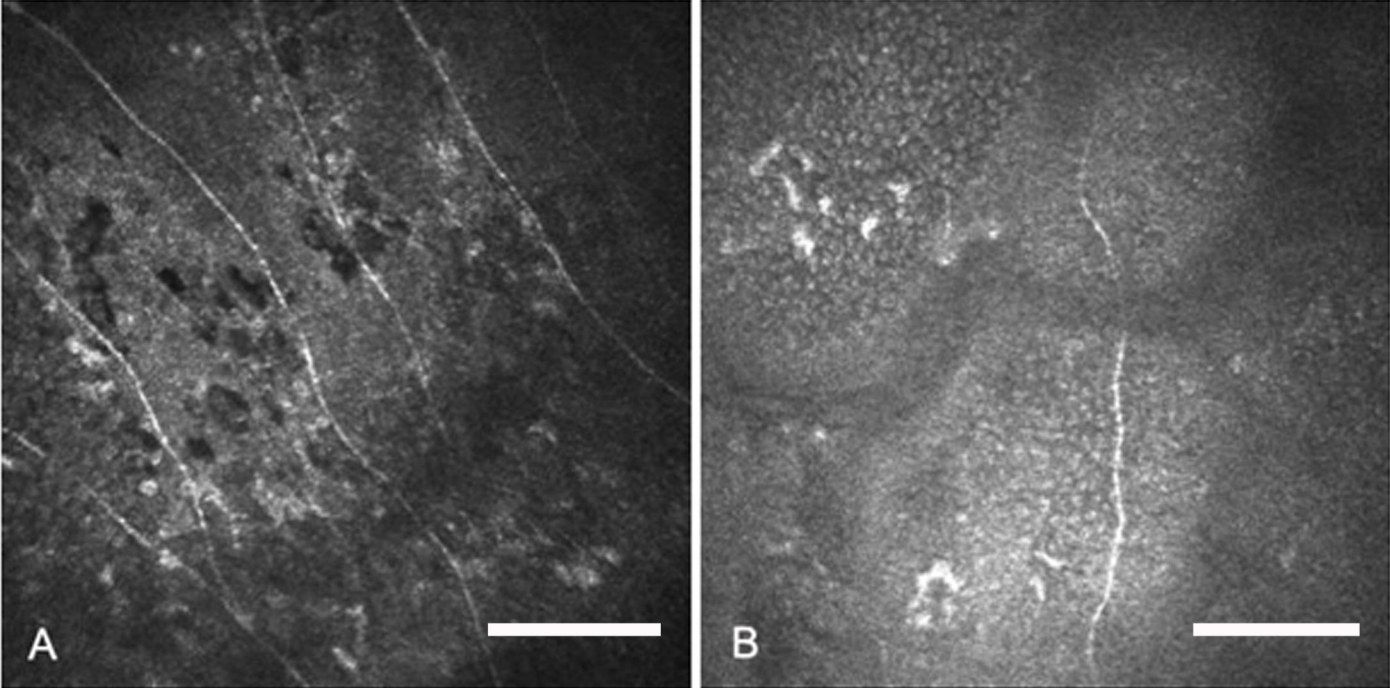
A
B

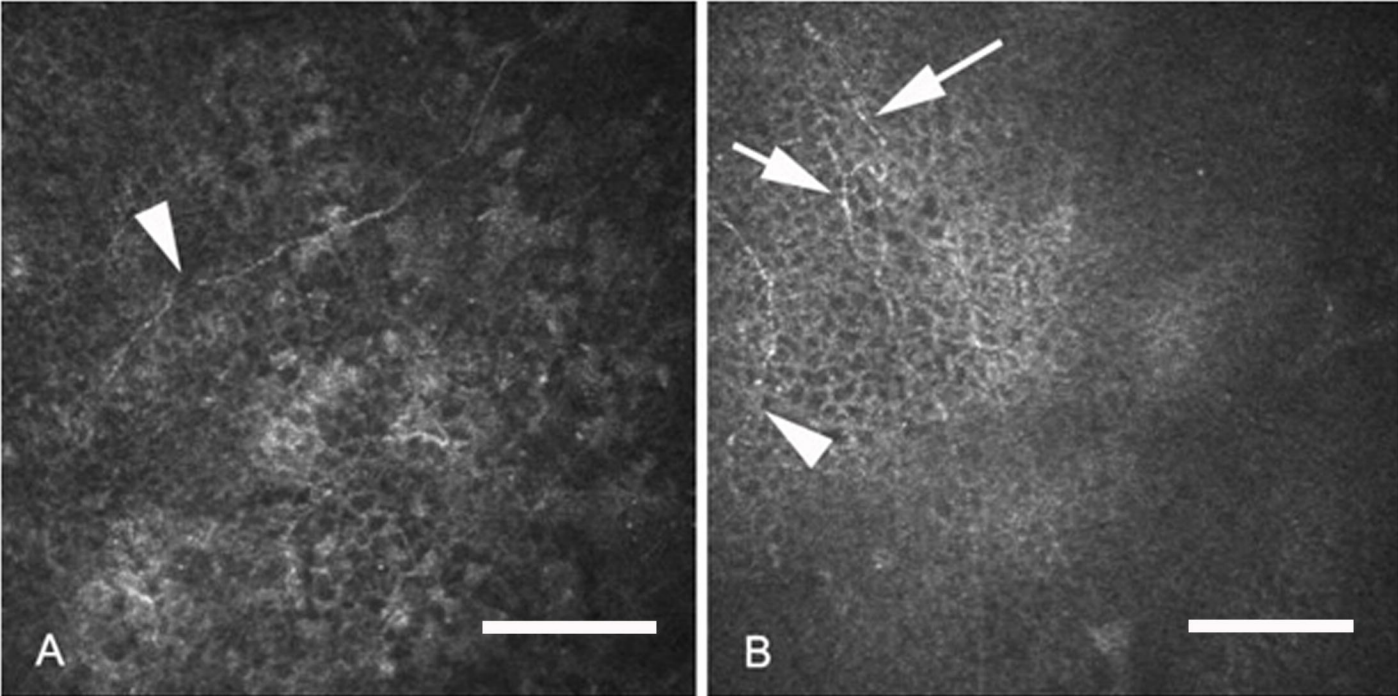
A
B

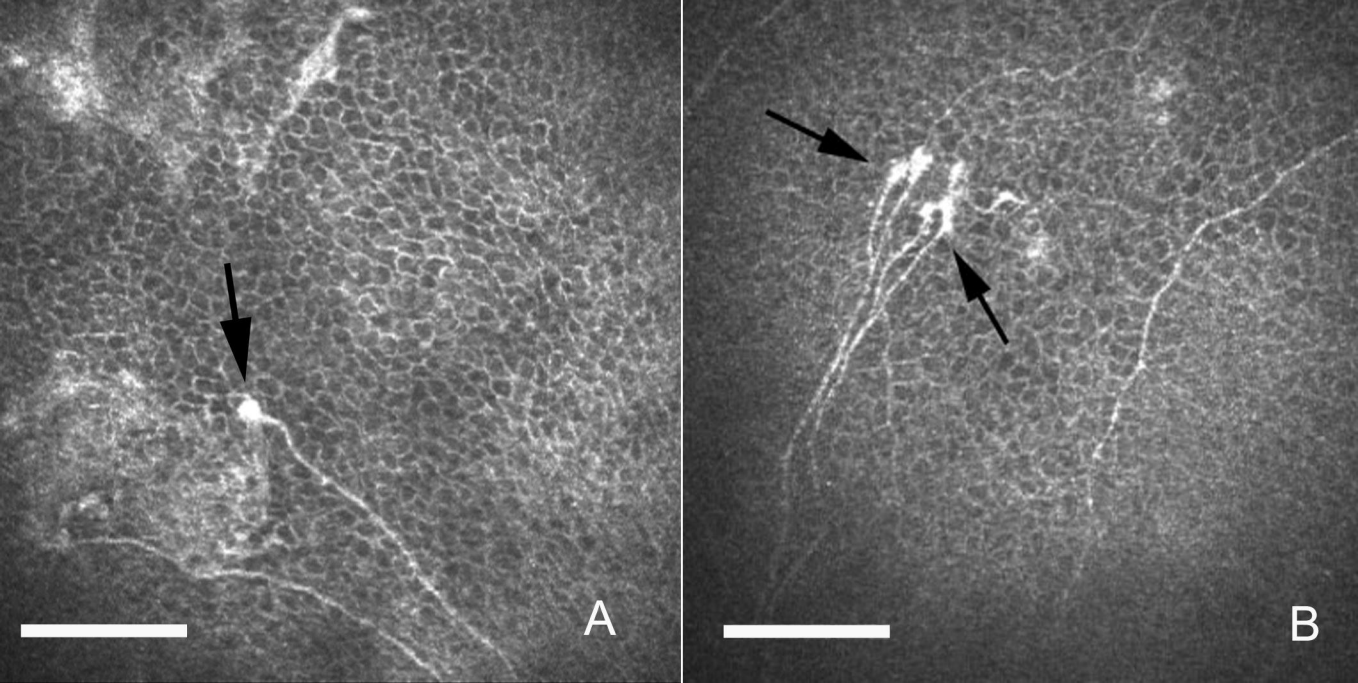
A
B

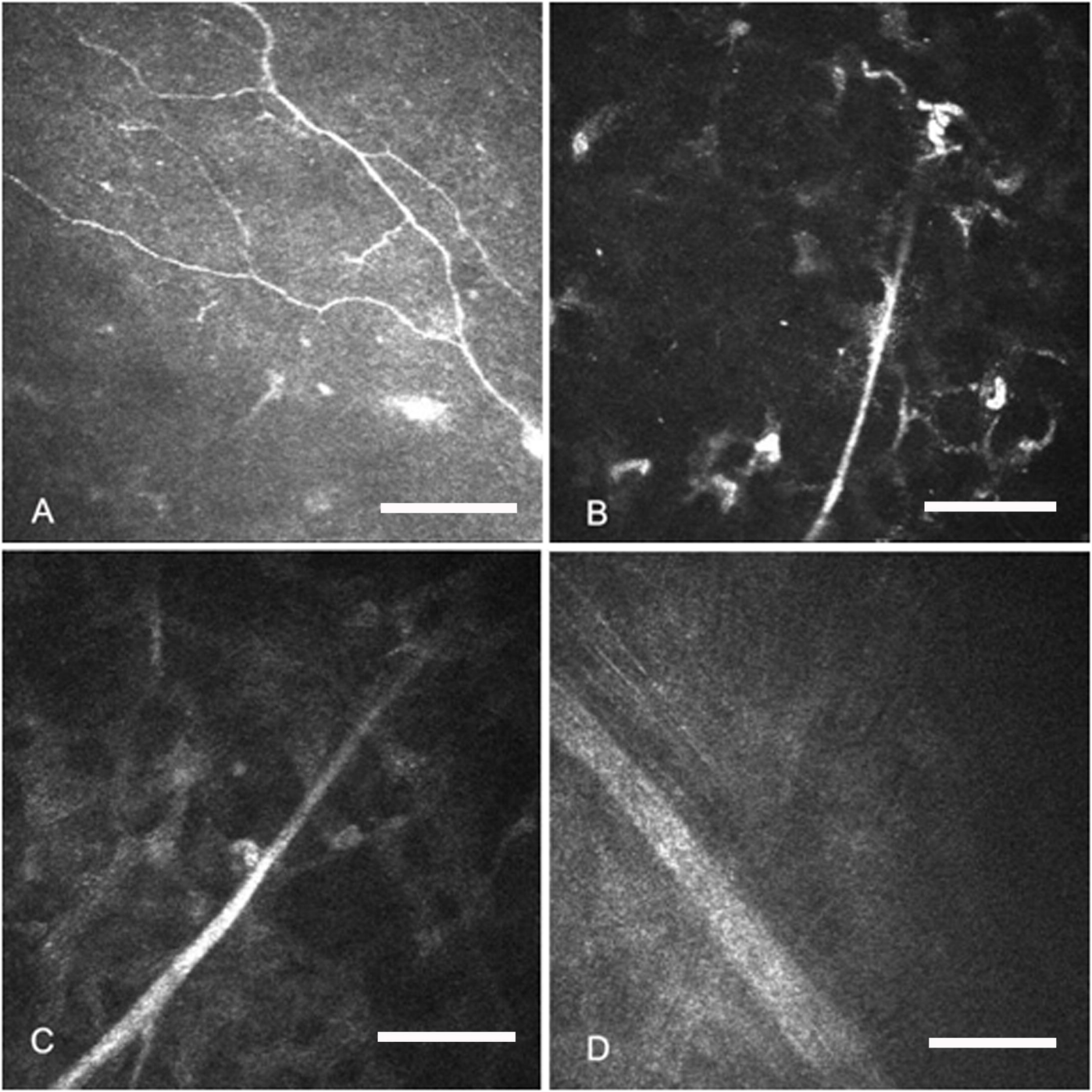
A
B
C
D


B|BRAUN
Cleansing
B|BRAUN